REPORT DOCUMENTATION PAGE

Form Approved
OMB No. 0704-0188

1. REPORT DATE *(DD-MM-YYYY)*	2. REPORT TYPE	3. DATES COVERED *(From - To)*
16-09-2002	Journal Article	3 Oct 1998 - 2 Aug 2002

4. TITLE AND SUBTITLE

Design and Commissioning of a Hi-Resolution Visible/Near-IR Echelle Spectrograph (HI-VIS) for the AEOS Telescope

5a. CONTRACT NUMBER
F29601-00-D-0204

5b. GRANT NUMBER
N/A

5c. PROGRAM ELEMENT NUMBER
63444F

6. AUTHOR(S)

Robert Thornton, Jeffrey Kuhn, Klaus Hodapp, Donald Mickey, Alan Stockton,

Tony Young, Everett Irwin
Mark Waterson, Gerald Luppino, Mike Mayberry, Hubert Yamada, Kent Fletcher

5d. PROJECT NUMBER
4868/4983

5e. TASK NUMBER
B3

5f. WORK UNIT NUMBER
BH

7. PERFORMING ORGANIZATION NAME(S) AND ADDRESS(ES)

AFRL/DEBI (Det 15)
535 Lipoa Parkway Ste 200
Kihei HI 96753

8. PERFORMING ORGANIZATION REPORT NUMBER

Det 15 AFRL 0222

9. SPONSORING / MONITORING AGENCY NAME(S) AND ADDRESS(ES)

10. SPONSOR/MONITOR'S ACRONYM(S)

11. SPONSOR/MONITOR'S REPORT NUMBER(S)

12. DISTRIBUTION / AVAILABILITY STATEMENT
Approved for public release; distribution is unlimited.

13. SUPPLEMENTARY NOTES Robert Thornton, Jeffrey Kuhn, Klaus Hodapp, Donald Mickey, Alan Stockton, Tony Young, Everett Irwin, Mark Waterson, Gerald Luppino, Mike Mayberry, Hubert Yamada, Kent Fletcher, "Design and Commissioning of a Dual Visible/Near-IR Echelle Spectrograph for the AEOS Telescope, " 2002 AMOS Technical Conference, Maui, Hawaii 16-20 September 2002.

14. ABSTRACT

The Institute for Astronomy has developed and recently installed a high-resolution cross-dispersed echelle spectrograph for use at one of the coude foci of the AEOS 3.7-meter telescope, operated by the Air Force Space Command atop Mt. Haleakala on the island of Maui. The spectrograph features an optical arm for the wavelength range 0.5-1.0 um and an infrared arm for the range 1.0 - 2.5um. We review the spectrograph design and present commissioning results obtained with both the visible and infrared arms. Both channels use a white-pupil collimator design to maximize grating efficiency and to limit the size of the camera optics. The visible arm of the spectrograph uses deep-depletion CCDs optimized for operation near 1.0 um. The infrared detector is a 2048 x 2048 hgCdTe array (HAWAII-2) that has been developed by Rockwell Science Center for this project. Both channels are equipped with slit-viewing cameras for object acquisition and control of a fast guiding tip-tilt mirror located in a pupil image in the spectrograph fore optics.

15. SUBJECT TERMS

AEOS, CCD, Institute for Astronomy

16. SECURITY CLASSIFICATION OF:			17. LIMITATION OF ABSTRACT	18. NUMBER OF PAGES	19a. NAME OF RESPONSIBLE PERSON
a. REPORT	b. ABSTRACT	c. THIS PAGE			19b. TELEPHONE NUMBER *(include area code)*
Unclassified	Unclassified	Unclassified	Unlimited	11	Klaus Hodapp (808) 932-2313

DESIGN AND COMMISSIONING OF A HI-RESOLUTION VISIBLE/NEAR-IR ECHELLE SPECTROGRAPH (HI-VIS) FOR THE AEOS TELESCOPE

Robert J. Thornton, Jeffrey R. Kuhn, Klaus W. Hodapp, Donald L. Mickey, Alan N. Stockton, Mark F. Waterson, Gerard A. Luppino, Mike Maberry, Hubert Yamada, Kent Fletcher, Tony Young, and Everett Irwin

University of Hawaii Institute for Astronomy, 2680 Woodlawn Drive, Honolulu, HI 96822

ABSTRACT

The Institute for Astronomy has developed and recently installed a high-resolution cross-dispersed echelle spectrograph for use at one of the coudé foci of the AEOS 3.7-meter telescope, operated by the Air Force Space Command atop Mt. Haleakala on the island of Maui. The spectrograph features an optical arm for the wavelength range 0.5 -1.0 μm and an infrared arm for the range 1.0 - 2.5 μm. We review the spectrograph design and present commissioning results obtained with both the visible and infrared arms. Both channels use a white-pupil collimator design to maximize grating efficiency and to limit the size of the camera optics. The visible arm of the spectrograph uses deep-depletion CCDs optimized for operation near 1.0 μm. The infrared detector is a 2048 × 2048 HgCdTe array (HAWAII-2) that has been developed by the Rockwell Science Center for this project. Both channels are equipped with slit-viewing cameras for object acquisition and control of a fast guiding tip-tilt mirror located at a pupil image in the spectrograph fore optics.

Keywords: infrared, spectroscopy, high-resolution, echelle, AEOS

1. INTRODUCTION

The sky background at long optical and near-infrared wavelengths is dominated by OH airglow emission. With sufficiently high spectral resolution, most of the spectrum is actually unaffected by these emission lines and the remaining natural continuum background is very low. As a consequence, the sensitivity achieved between the OH airglow lines is detector noise- and dark current-limited in most existing instruments. If detectors have sufficiently low noise and dark current to allow a background limited detection of the high-resolution spectrum over a wide free spectral range, the OH lines can simply be masked off in data reduction and the spectrum of the object can be extracted from the pixels between the lines. This approach is certainly feasible in the optical with modern CCDs having less than 2 electrons noise and negligible dark current. Existing infrared arrays have demonstrated read noise of less than 5 electrons rms (Hodapp et al. 1996) and dark current accumulation of less than 1 electron/minute, close enough to the noise criteria to use this approach in the infrared.

The visible detector uses a mosaic 4096 × 4096 thinned CCD array, providing coverage of the wavelength range 0.5--1.0 μm in two settings with a maximum resolving power of ≈ 50,000. The near-infrared detector is a Hawaii-2 2048 × 2048 HgCdTe array from the Rockwell Science Center. This large-format detector will permit coverage of the entire *J* or *H* band in a single grating setting and coverage of the *K* band in two settings. The spectral resolution will be approximately 30,000 with a 2-pixel-wide slit. The combination of wide simultaneous spectral coverage and high spectral resolution will make this instrument competitive with current 8-m class instruments for many types of observations.

To actually achieve the low background levels expected between the OH airglow lines, it is essential that stray light from intense lines be minimized. Our experience with the low-resolution spectrograph KSPEC and other infrared instruments built at the IfA have given us confidence that the required suppression of stray light can be achieved. The AEOS spectrograph design also includes an image rotator, and provides adequate separation between adjacent echelle orders in both channels so that it will be possible to obtain spectra of faint, moderately extended objects while still allowing for sky subtraction. Finally, "tip-tilt" compensation for seeing-induced image motion is provided to maximize throughput through narrow slits.

2. OPTICAL DESIGN

2.1 Overview

The large-format array detectors used provide wide wavelength coverage at high spectral resolution. However, they place severe demands on the optics following the echelle gratings because of the large range of angular dispersion required. Classical echelle designs lead to compromises that reduce throughput and require large, expensive and complex camera optics. The so-called "white pupil" design used in this instrument solves most of these problems, allowing the spectrograph camera optics to be smaller and less complex and the echelle to be used very close to true Littrow configuration. Similar designs have been used in a number of spectrographs, most notably in the UVES system built by the European Southern Observatories for the VLT 8-m telescope. In two-mirror white pupil spectrographs, a second collimator mirror allows placing the pupil image on both the echelle and the cross-disperser gratings, thus minimizing the size of the spectrograph camera optics. In the AEOS spectrographs, a single large mirror serves as the collimator for both the echelle and cross-disperser gratings and as the intermediate imager. Light from the entrance slit is collimated by the spherical mirror, forming a pupil image on the echelle. The dispersed light is imaged into a spectrum - with all the orders superimposed - on a flat mirror between the two gratings. A second reflection from the spherical collimator mirror recombines the spectrum into a single pupil image (the "white pupil") on the cross-disperser, which separates the orders. A refractive camera system images the spectrum onto the detector.

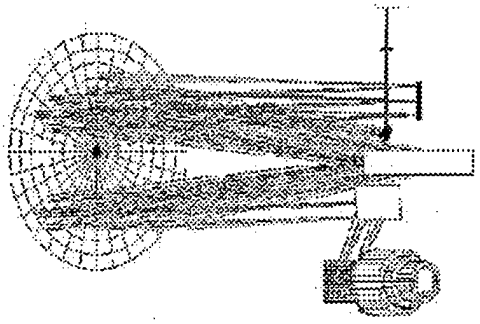

Fig. 1: Optical ray-trace of the white pupil spectrograph design.

The instrument consists of three major sections (Fig. 1): the common fore optics, the visible spectrograph, and the infrared spectrograph. The beam from the common optics is directed to the visible spectrograph by a pick-off mirror mounted on a linear stage. When the pick-off mirror moves out of the light beam, the light is fed to the IR spectrograph. This mirror could be replaced with an IR-transmitting dichroic, permitting both the IR and visible spectrographs to be used simultaneously.

The AEOS coudé beam proceeds vertically downward along the telescope azimuth axis to the coudé level, where it is reflected into one of seven separate experiment areas by a steering mirror. Each experiment area is separated into an inner "Optics Room", and a larger outer room called the "Experiment Room". The complete optical system is housed within one of the Optics Rooms (Fig. 1) along with the minimum amount of electronics that must be close to the detectors. The remaining electronics, vacuum and thermal equipment are located in the adjacent Experiment Room. The location of the f/200 focal plane near the center of the rear Experiment Room required us to insert several fold mirrors ahead of the re-imaging optics, as indicated in Fig. 2. A spherical mirror of 5.5m focal length, located 5.5 meters behind the f/200 image plane, collimates the image and forms a 28-mm diameter pupil image. The image rotator is a conventional three-mirror system, with the first and last mirrors replicated onto a monolithic aluminum wedge. Once adjusted so that the desired position angle on the sky is aligned with the spectrograph slits, it is controlled to keep that position angle constant as the telescope tracks. A small fold mirror follows to locate the pupil image on the tip-tilt mirror. The tip-tilt stage is a 1-inch diameter piezo-electric 2 axis platform manufactured by Polytech - Physik Instrumente. The platform's +/- 1-milli-radian angular range compensates for seeing-induced image motion within three arcsec of the nominal image position; image motion beyond this range is corrected by stepping the telescope. Following this mirror, a 1.1-m focal length spherical mirror forms a second image at f/40 on

the entrance slits of the spectrographs. A short distance in front of this secondary focal plane, a pick-off mirror mounted on a linear stage directs the beam to the optical arm, or, moved out of the light path, allows the beam to proceed to the IR arm. A calibration unit containing a Thorium-Argon hollow cathode lamp for spectral calibration and a quart halogen lamp for producing flat-field images is also located in the fore optics section. A diffusing screen switches between the calibration sources and the sky. All mirror surfaces are coated with enhanced silver for its high reflectivity over a broad wavelength range.

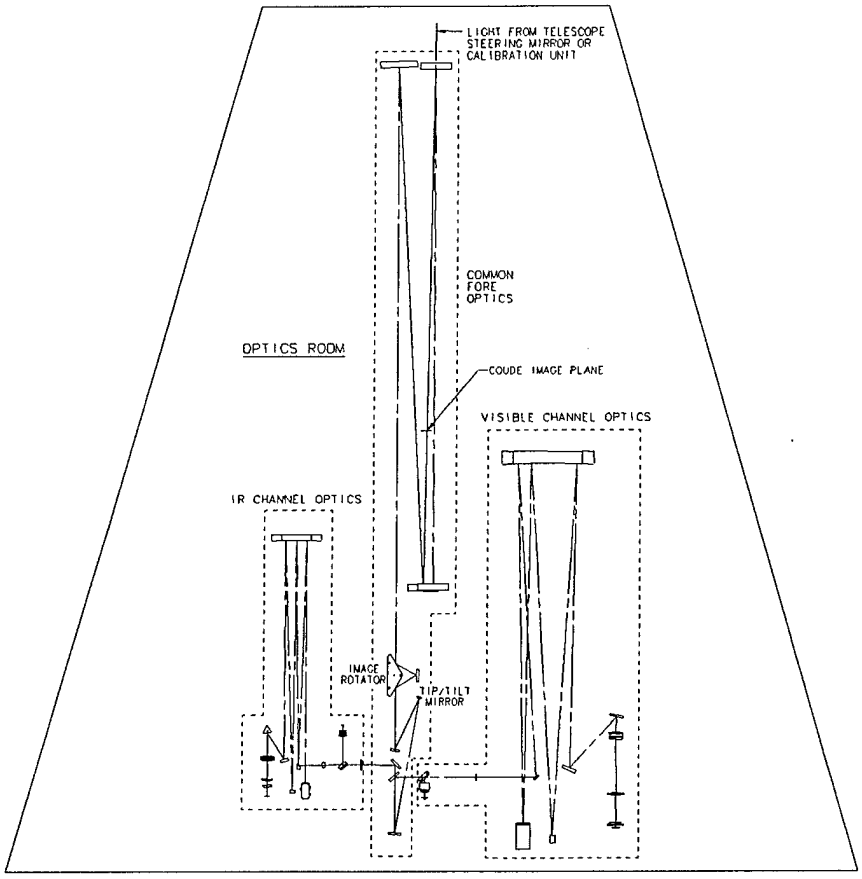

Fig. 2: Optical path in the AEOS spectrograph: The three major components are the common fore-optics, the visible spectrograph channel, and the infrared spectrograph channel.

2.2 Spectrograph Optical Characteristics

The two spectrograph sections share a common design and are scaled by wavelength, resulting in similar spectral resolution at the respective detectors. A selection of different slit widths and binning modes allow the instrument's performance to be optimized for a given observation by trading spectral resolution for light transmission. We envision several primary modes of operation:

- For stellar spectroscopy at moderately high resolution, a 0.35 arcsec slit projects to two pixels at R ≈ 49,000.
- A 0.7 arcsec slit, projecting to ≈ 6 pixels at R ≈ 25,000, gives better sampling of the projected slit profile, especially useful for projects for which accurate subtraction of airglow lines is critical.
- For faint objects, a 1 arcsec slit, used with 2X binning on the CCD, gives R ≈ 16,500. This resolution is still sufficient for strong OH airglow lines to obscure only a small fraction of the spectral range.

Table 1: Visible and IR Spectral Resolution

Slit Width (arcsec)	Slit Width (linear mm)	Resolution
0.35	0.250	48,900
0.71	0.506	24,500
1.00	0.715	17,100
1.50	1.071	12,800
2.00	2.849	8,500

2.3 Visible Spectrograph

When the common optics visible pickoff mirror is inserted, the f/40 beam entering the spectrograph is imaged onto a slit mirror. The reflected beam from the slit mirror is re-imaged onto a commercial SBIG STV 512×512 CCD camera using a 28-mm f/1.4 Nikon lens. The camera is used for tip-tilt guiding as well as monitoring the slit image.

Basic visible channel characteristics:

Image Scale at detector:	0.125 arcsec / pixel
Wavelength range:	0.5 – 1.0 μm with 2 cross-dispersion gratings
Detector mosaic:	2 – 2048 x 4096 deep depletion CCDs, 15-μm pixels

The visible section of the spectrograph uses a white-pupil design with a 75 mm collimated beam. The 520 mm focal length camera gives an image scale of 0.125 arcsec per pixel on the CCD array. Several slits (Table 1) are available in a slit wheel. The beam from the collimator mirror passes to a fixed echelle grating with 52.6 grooves per mm and a 65.0-degree blaze angle. The beam returns to the collimator mirror, now acting as a camera, which images the spectrum (all orders combined) onto a flat mirror. From the mirror, the diverging beam returns to the collimator, which once again collimates the light and images the pupil onto one of the two interchangeable cross-dispersing gratings optimized for redder and bluer wavelength ranges (Table 2). The spectrograph camera lens is a five-element, 0.75-m long air-spaced design developed at the IfA. Overall image quality is dominated by the off-axis reflections at the collimator mirror. All mirrors have enhanced silver coatings, and all transmission surfaces have broadband antireflection coatings.

Table 2: Visible Cross-Disperser Characteristics

λ Coverage	Ruling	Blaze λ	Order	Echelle Orders
0.50 - 0.77μm	384 l/mm	0.61 μm	1	45 - 69
0.64 - 1.00 μm	300 l/mm	0.86 μm	1	34 - 53

2.4 Infrared Spectrograph

Basic IR channel characteristics:

Image scale at detector:	0.16 arcsec/pixel
Wavelength range:	1.0 - 2.5 μm with 3 cross-dispersion gratings
Slit-viewing detector:	HAWAII 1K x 1K, HgCdTe
Science detector:	HAWAII 2K x 2K, HgCdTe, 18-μm pixels

The optical design of the infrared spectrograph is very similar to that of the visible channel. The f/40 beam entering the spectrograph is imaged onto a slit mirror identical to those in the visible channel. The entire 1 arcmin diameter field is reflected from the slit mirror (as in the visible channel), passes through a filter wheel, and is re-imaged onto one quadrant of a 1024 × 1024 HAWAII array (i.e., a 512 × 512 sub-array) at a scale of 0.12 arcsec per pixel. This scale is well suited for fast sub-array reads for tip-tilt guiding.

Light passing through the slit is band-limited by *J*, *H*, or *K* filters immediately behind the slit, then directed by a small fold mirror to the 2-m focal length collimator. The beam then encounters in succession the echelle, the

collimator, the flat mirror at the intermediate image plane, the collimator again, and finally the cross-disperser and the camera. The camera optics consist of a four-element refractive system with a focal length of 307 mm, optimized for resolution over the full detector area wavelength range and for minimum reflection ghosts. Particular attention has been paid to reflections from the surface of the detector. The worst ghost is a double reflection between two lens surfaces, all of which are anti-reflection coated. We estimate an average total transmission of ~ 7% for the entire optical train, from the telescope primary to science detector.

Table 3: Infrared Cross-Disperser Characteristics

Grating	Ruling	Blaze Angle	Order	Echelle Orders
J	400 l/mm	15.0°	1	42-51
H	300 l/mm	14.8°	1	31-39
K	200 l/mm	15.0°	1	24-30

3. MECHANICAL AND THERMAL DESIGN

3.1 Overview

Fig. 3shows a 3-D layout of all the mechanical components of the spectrograph (corresponding to the optics layout in Fig. 2). The common fore optics are divided between two central optical benches, a 4 ft. x 6 ft. bench at the front of the optics room on top of which rests the calibration unit, and a narrow 30 in x 8 ft "aft" table. Most of the visible channel components fit on a 5 ft. x 12 ft x optical table; the visible guider assembly is mounted on the aft common optics table. The infrared dewar is supported by a welded steel frame providing necessary .adjustment to allow co-aligning the two spectrograph channels.

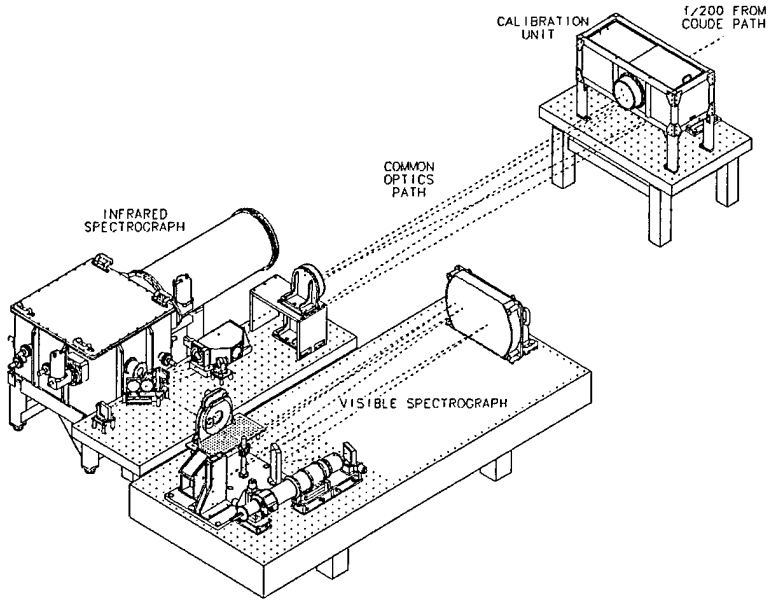

Fig. 3: Overall opto-mechanical layout of the AEOS spectrograph (light/dust cover assembly is not shown).

The designs of mechanical assemblies for the visible channel were straightforward. There are eight motorized mechanisms required for the visible channel. Except for the slit wheel, all were commercial stepper motor stages purchased from NEAT (Kollmorgen). The slit wheel is a 12-position Geneva mechanism designed in-house for precise position repeatability and driven by a Phytron motor (Bell et al. 1998). The other mechanisms include a rotary stage for switching between the two cross-dispersers, a linear stage for focusing the spectrograph camera lens,

and an X-Y stage for translating the CCD dewar (in case a target spectral feature happened to fall on the ≈ 0.25 mm gap between the two detectors of the mosaic).

The infrared cryostat maintains the temperature of all optics downstream of the IR pickoff mirror, mechanisms, and detectors at or below ≈ 77 K. Although including the collimator mirror in the cryostat reduced emissivity contributions, it also meant an approximate doubling of the size of the cryostat and vacuum jacket volumes and additional alignment and structural challenges. The resulting total cold mass is approximately 200 kg. The infrared mechanical structure was designed around the optical layout, iterations for both being made to keep the overall instrument envelope and mass as small as possible.

3.2 IR Spectrograph Vacuum Jacket

The size of the required vacuum jacket made forging a monolithic aluminum structure, as was done for previous large infrared instruments built at the IfA, both costly and time-consuming. Among the other options available, we chose to have an outside vendor TiG weld the structure from stainless steel 304L components. There are two main sections to the vacuum jacket structure: a box structure containing the cold plate and most of the cryostat assemblies, and a tubular snout extension through which an inner, cold collimator mirror support tube projects. The main cubical section was fabricated by welding individual 3/8 in stainless steel plates together. The collimator tube, whose geometry made it inherently better able to withstand external atmospheric pressure, was rolled from one ¼ in plate and sealed with one weld along the length of the tube. The number of welds was minimized to reduce heat input and subsequent stresses within the structure. The two main sections of the vacuum jacket are bolted together and O-ring sealed, as are the access covers to each section. Exterior strengthening ribs welded onto the main section were required for structural stability. Extensive finite element analyses (FEA) demonstrated that all deflections of the vacuum jacket due to atmospheric pressure are much less than 1 mm. The mass of the completed vacuum jacket is approximately 200-kg (without internal optics).

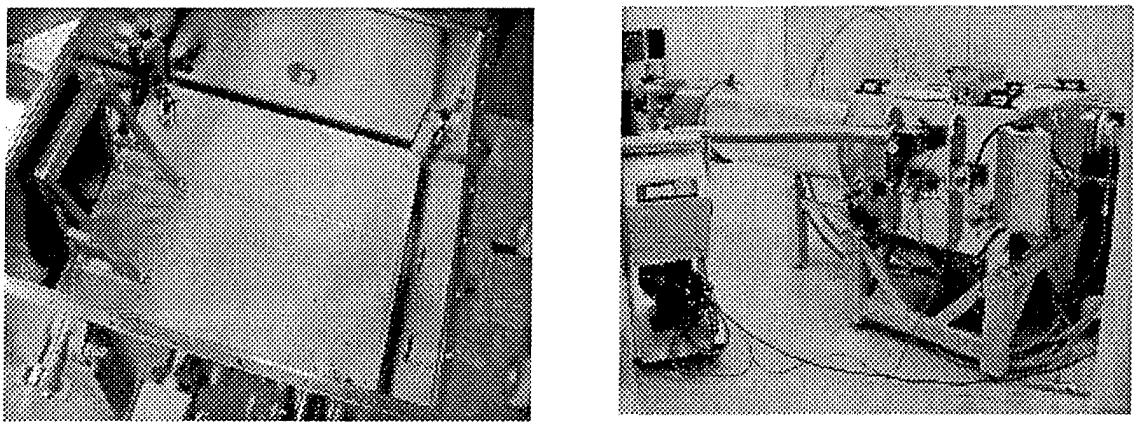

Fig. 4: The left-hand picture shows the inside of the main section of the vacuum jacket. The main mounting surface is attached to the inside of the jacket structure via four titanium standoffs at the corners designed to accommodate shrinkage of the work surface. Also visible is the wallpaper shield hugging the inside surface of the vacuum jacket as well as the bracket onto which the inner, cold cryostat collimator tube attaches. The picture on the right shows the infrared spectrograph installed in the AEOS facility.

3.3 Thermal Design

The cryostat is cooled via two Leybold Coolpower 110S closed-cycle helium cryogenic refrigeration systems with water-cooled primary compressors chosen based on successful experience with a similar cooling system for the NIRI instrument (Hodapp et al. 1998), whose cold mass was 1.5-2 times that of this instrument. The total heat load on the coolers was estimated to be 75 Watts, while each cryo-cooler includes two refrigeration stages that provide a total cooling capacity of 130 Watts. The two first stages are connected to the cold plate by oxygen-free high-

conductivity (OFHC) copper straps and cool all of the cryostat mass, including the collimator tube. One of the second stage units is used for cooling the Hawaii 2 science array to ≈ 60K, while the other cools the Hawaii 1 slit-viewer array to ~ 70K and has a charcoal getter attached.

The design of the shielding for the cryostat was also based on earlier instruments designed at the IfA. A highly polished stainless steel wallpaper shield covers the inside surfaces of the main section of the vacuum jacket, but is thermally isolated from it. Ideally, a gold floating shield would have been even less emissive, however the cost advantage in using stainless steel was considerable. A cold inner radiation shield structure attached directly to the work surface is also provided to intercept thermal radiation from the warm vacuum jacket shielding the cold optics. Layers of 0.05 mm thick metalized Mylar radiation shielding were added to the inside of the tube extension after long cool down times for the collimator mirror were observed during preliminary testing.

3.4 Cryostat Internal Design

The IR spectrograph includes seven moving mechanisms inside the dewar (Fig. 5): a slit wheel, a slit-viewer filter wheel, a slit-viewer lens focus stage, a science channel filter wheel, an echelle grating tilt-stage, a cross-disperser turret, and a science detector focus stage. All cold mechanisms are driven by Phytron "cryo-vac" stepper motors. Based upon previous cryogenic instruments developed at the IfA, the mechanism drive trains use either ball bearings modified for cryogenic use or Vespel bushings for support. Ball bearings have the advantage of offering more precise positioning, though they run the risk of jamming more easily. Vespel bushings offer the advantage of providing a small amount of self-lubrication, but their large differential contraction (1.7 %) from ambient to cryogenic temperatures can create problems. All mechanisms except for the two filter wheels use Hall Effect sensor packages for position sensing and calibration while the filter wheels rely upon mechanical limit switches.

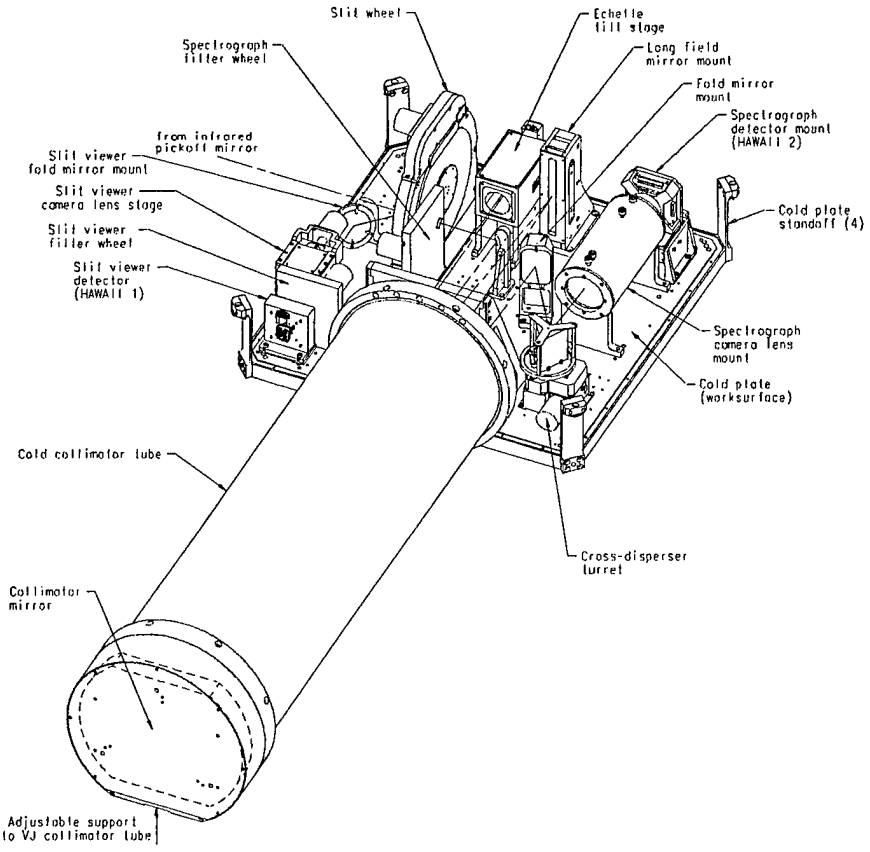

Fig. 5: The primary interior components of the cryostat (radiation shields, cooling system, baffling, etc. not shown for clarity).

4. ELECTRONICS AND SOFTWARE

The spectrograph detectors, electronics and mechanical devices are controlled by software hosted on three Linux PCs, while system monitoring and quick-look data analysis programs are available on a Sun workstation. The software system is written in Tcl/Tk with necessary C support functions.

The computers and all major electronic components are located in the outer experiment room to provide minimal heat loading into the areas containing the optical system. Power and control cables run through a light seal and cable restraint clamp plate closing off the port connecting the two coudé rooms, allowing local operation of the instrument under normal lighting conditions. Compressor/heat exchanger units for the closed-cycle cryogenic coolers are also located in the outer experiment room.

4.1 Instrument Control

Control of system mechanisms is implemented using commercial 8-axis motor controllers from Galil Motion Control and micro-stepping motor drivers from Phytron. Internal cold mechanisms are driven by Phytron cryogenic stepper motors while external mechanisms use commercial motion stage assemblies from New England Affiliated Technologies. Graphical user interfaces are provided to control the mechanisms for instrument setup and operation.

The IR channel cryostat is equipped with five temperature sensors to monitor internal temperatures at various locations. Three are used with Omega CYC3200 controllers to stabilize important locations in the cryostat: (1) the center of the cold plate, (2) the science detector, and (3) the slit-viewer detector. The remaining two sensors can be optionally placed at other useful locations to monitor thermal gradients. The temperature control system ensures that all detector arrays are maintained at a higher temperature than their surrounding environment during operation and warm-up to prevent contamination. A computer-independent auto-shutdown and inter-lock safety system was designed to prevent overheating of cryostat components should any of the heater systems fail. On-line display of temperatures allows remote monitoring of the system during cooling and warm-up.

4.2 Detector Readout

The detectors for both the visible and IR channels are controlled by San Diego State University "Leach Generation-2" DSP-based controllers with IfA-customized software for both array readout and display. The readout electronics enclosures are located adjacent to each of the detectors (external to the dewar) and signals are brought out to the control computers on fiber-optic links. The controllers utilize Motorola digital signal processors to generate array clocks, trigger digitization of array output, and process image data for transmission to the host computer. In addition, custom DSP code running on the IR slit-viewing array controller calculates the centroid of a guide-star and directly drives the tip-tilt mirror to provide image drift correction.

5. TESTING AND PERFORMANCE ASSESSMENT

We are currently in the commissioning phase of the project. Observations of stellar objects with the visible channel are routinely undertaken at present. Testing and calibration work continues on the IR channel. We summarize here early testing and performance data obtained.

5.1 Visible Channel

One of the first spectrograms obtained with the full 4K x 4 K mosaic focal plane array was of the Moon (Fig. 6, below) . This spectrum was taken with the blue grating before final alignment and calibration, so only about15 of the $\approx$ 22 intended orders are visible, spanning approximately 6800 Å to nearly 9000 Å from top to bottom. It was acquired before final alignment but shows a clear cross-dispersed spectrum, including many solar and telluric lines.

The first spectral standard star reduced was HR1544, a V=4.35 A0V star. Observations were taken in both slit- and slitless modes; the slitless data were used for efficiency estimates. Fig. 7 below shows all of the extracted orders after flux calibration compared with flux values from the literature. The average efficiency over the wavelength range is about 7%, as predicted.

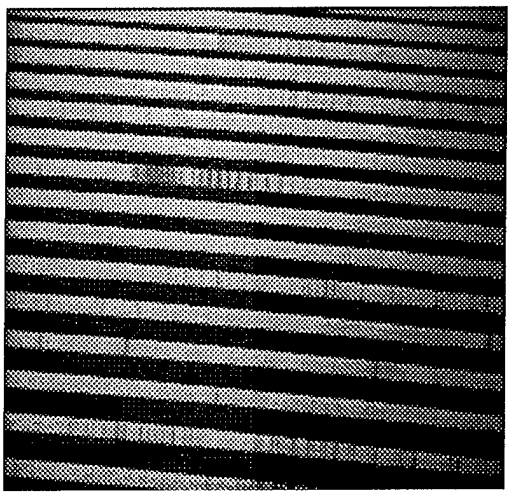

Fig. 6: Lunar echellogram, 0.7 arcsec slit, binned 2x2.

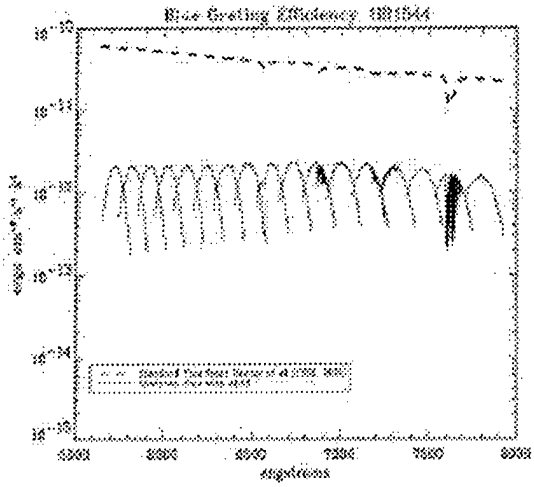

Fig. 7: Estimate of visible spectrograph sensitivity from slit-less observations of standard star HR1544.

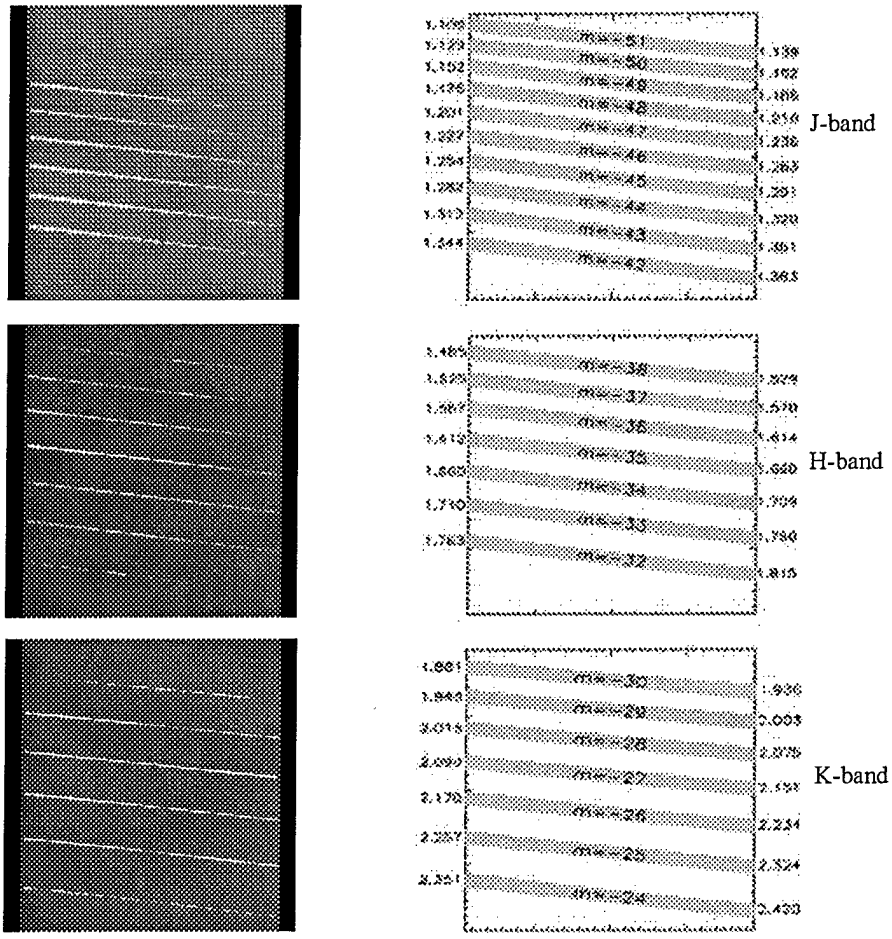

Fig. 8 *J*, *H*, and *K* echellograms of Arcturus (left) compared to the planned order layout/wavelength coverage (right).

5.2 Infrared Channel

The infrared channel was delivered to the AEOS telescope in April 2002, and is still undergoing final testing. The first *J*, *H*, and *K* echellograms of Arcturus obtained with the IR channel are shown in Fig. 8. Expected wavelength coverage and order locations were achieved, although several issues still need to be addressed. For example, the right-to-left variations in the *J* and *H* spectrograms are most likely due to slight misalignment of the echelle and or/collimator. The smear in the middle of the *K* echellogram was due to a light leak within the cryostat and has since been rectified. We are in the process of obtaining throughput estimates with recently acquired data.

6. CONCLUSIONS

The commissioning tests underway on the AEOS high-resolution visible/infra-red spectrograph show that the instrument will meet its design objectives and provide a valuable resource to the AEOS facility. The instrument will be useful for a wide range of scientific investigations requiring high spectral resolution and wide wavelength coverage.

The most distinguishing features of the AEOS Spectrograph are its high-resolution, low detector-noise, and wide spectral coverage (0.5 - 2.5 μm). The IR channel is one of the highest resolution infrared spectrographs in existence on a 4 m or larger class telescope. The wide spectral coverage is useful for any science requiring synoptic observations. There are a number of scientific programs, covering a broad range of interests, that could benefit from these instrument features. Over the past decade, the field of star formation regions and young stellar objects has evolved particularly rapidly. These environments typically have high opacities at short wavelengths, making them attractive targets for the low-noise 2K HAWAII IR array. Related to this is the spectral classification of ultra-cool stars, e.g., L and T dwarfs, many new features of which are currently being discovered with medium- to high resolution infrared spectrographs. Another related field well matched for AEOS is searching for low-mass stellar and sub-stellar companions of stars involving radial velocity studies over long timescales. Studies of stellar oscillations will also be possible with the instrument.

ACKNOWLEDGEMENTS

This work was supported by the Air Force Research Laboratory under contract # F29601-96-C-0125.

REFERENCES:

Bell, J. et al. 1998, SPIE 3354, 1103
Hodapp, K.-W. et al. 1996, New Astronomy 1, 1777
Hodapp, K.-W. et al. 2000, SPIE, 4008, 778
Hodapp, K.-W. et al. 1998, SPIE, 3354, 545
Hamuy, M. et al.1994 PASP, 106, 566
Iwamuro, F. et al. 1994, PASJ, 46, 515
Kozlowsky, L. J. et al. 1998, SPIE 3354, 66
Tokunaga, A.T. et al. 1998, SPIE 3354, 512
Young, T. et al. 1998, SPIE, 3354, 317